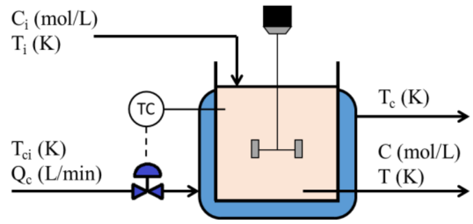

Fig. 1. Schematic diagram of the CSTR process.

1 Interpretable Incipient Fault Detection and Isolation with Cauchy-Schwarz Divergence

In the following, we perform experiments on the continuous stirred-tank heater (CSTH) process to demonstrate the interpretability of conditional CS divergence based fault isolation.

1.1 Application to CSTR Process

This section discusses the effectiveness of the proposed method in a closed-loop continuous stirred-tank reactor (CSTR) process, which is a common chemical system that designed especially for simulating incipient faults [1], [2], [3], [4]. The dynamic characteristics of CSTR process is described by mass balance and energy conservation,

$$\frac{dC}{dt} = \frac{Q}{V}(C_i - C) - akC + v_1, \tag{1}$$

$$\frac{dT}{dt} = \frac{Q}{V}(T_i - T) - a\frac{(\Delta H_r)kC}{\rho C_p} - b\frac{UA}{\rho C_p V}(T_i - T) + v_2, \tag{2}$$

$$\frac{dT_c}{dt} = \frac{Q_c}{V_c}(T_{ci} - T_c) + b\frac{UA}{\rho_c C_{pc} V_c}(T_c - T) + v_3, \tag{3}$$

where the input is $\mathbf{u} = [C_i, T_i, T_{ci}]^T$, the output is $\mathbf{y} = [C, T, T_c, Q_c]^T$, v_i is process noise, and k is an Arrhenius-type rate constant with $k = k_0 e^{(\frac{-E}{RT})}$. It is worth noting that, input disturbances can bring out system dynamics, such that measurements are temporally correlated, non-Gaussian-distributed and noisy due to the process non-linearity.

TABLE 1
Parameter description in CSTR process.

Parameter	Description	Value
Q	Inlet flow rate	100.0 L/min
V	Tank volume	150.0 L
V_c	Jacket volume	10.0 L
ΔH_r	Chemical reaction heat	-2.0×10^5 cal/mol
UA	Heat transfer coefficient	7.0×10^5 $cal/min/K$
k_0	Pre-exponential factor to k	7.2×10^{10} min^{-1}
E/R	Activation energy and gas constant	1.0×10^4 K
ρ, ρ_c	Fluid density	1000 g/L
C_p, C_{pc}	Fluid heat capacity	1.0 $cal/g/K$
v_1, v_2, v_3	Gaussian noise	$N(0, 0.01)$

The CSTR schematic in Fig. 1 shows the measurement locations and the control strategy: reactor temperature T is maintained by manipulating the coolant flow rate Q_c. In this application, we use the Simulink model developed by Pilario [2], available at https://www.mathworks.com/matlabcentral/fileexchange/66189-feedback-controlled-cstr-process-for-fault-simulation, details of parameters are described in Table. 1. The sampling interval is 1 min, 2000 points under normal conditions are collected as training data. Six variables are measure, $\mathbf{x} = [C, T, T_c, Q, C_i, T_i]^T$.

To evaluate the statistical power of CS divergence, 100 faulty data sets are generated from each scenario as Table. 2 shown, differing in the random seeds for process noise, measurement noise, and input disturbances. All testing sets have 1600 samples, with faults imposed since sample 201. Performance metrics for monitoring are averaged across all trials, the detailed results of FDR, FAR, and FDD are shown in Table. 3. As can be seen, most of methods have the FAR of 0 but not too early times of FDD, which suggests that an efficient way to reduce FDD deserves more investigations. Our proposed method obtains stable performance on all data sets in the sense that it has no failing cases, and even achieves compelling performance among others methods, demonstrating the effectiveness of CS divergence in distinguishing faulty

TABLE 2
Incipient fault scenarios in CSTR process.

Fault ID	Description	Value of f	Type
f_1	$Q = Q_0 + \delta$	5	Additive bias
f_2	$a = a_0 exp(-\delta t)$	0.0005	Multiplicative
f_3	$b = b_0 exp(-\delta t)$	0.001	Multiplicative
f_4	f_1, f_2 simultaneous		Multiplicative
f_5	$C_i = C_{i,0} + \delta t$	0.001	Additive
f_6	$T_{ci} = T_{ci,0} + \delta t$	0.05	Additive
f_7	$C = C_0 + \delta t$	0.001	Additive
f_8	$T = T_0 + \delta t$	0.05	Additive
f_9	$T_i = T_{i,0} + \delta t$	0.05	Additive
f_{10}	$Q_c = Q_{c,0} + \delta t$	-0.1	Additive

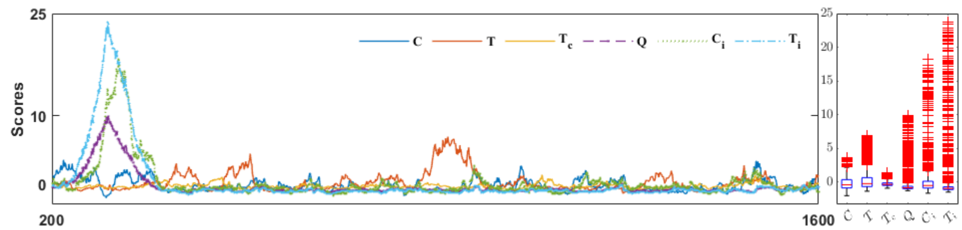

Fig. 2. Fault isolation results of f_1 for CSTR process.

states from normal distribution. Compared with classical SMD, our method has no false alarms for f_1 and f_2; and has a good detectability of 92.64% for f_9, whereas SMD failed to detect it.

For fairness, we have incorporated the projection of PCA to both SMD and our algorithm, aligning with the Wasserstein distance method. After subspace projection, there is a significant improvement in shortening the detection delay of our proposed method. The bias fault f_1 is identified at sample No.203, significantly earlier than the monitoring statistics of SMD (No.228) and Wasserstein distance (No.220). The average FDDs of our approach are 130, 133 and 60, especially the residual space can detect faults earlier than the SMD and WD based methods, highlighting its potential in incipient fault detection. In actual chemical engineering, timely detection of incipient faults can eliminate dangers at an early stage and maintain process safety.

For interpretability verification, we first evaluate the proposed fault isolation method on f_1, a sensor bias fault of 5 L/min is introduced to Q, corresponding to 201-th sample. f_1 is an incipient fault since the bias $5L$ is small compared with the initial value $330.9L$. If we look deeper, the conditional CS divergence is shown in Fig. 2. It presents the online sample-by-sample isolation result, we can observe that dimensions of Q, C_i, T_i are most related to the fault. This makes sense, because the dependence between Q and $\{C_i, T_i\}$ are shown in Eq. (1) and Eq. (2). It can be confirmed from the box-plot on the right that a large number of outliers appeared in these variables, and are concentrated on larger values, making the distribution right skewed.

Then we plot the result of monitoring based on conditional CS divergence in Fig. 3. From Fig. 3(a), the alarm points forming 8 phased stages. Their dependencies remain roughly the same in time period $[200, 303]$ (ascending) and $[302, 524]$ (descending), corresponding to Fig. 3(b). The 2-th dimension, controlled object T, contributes significantly to the 3-th stage due to the changes of its dependence structure Q. Therefore, our method provides more interpretability for dynamic monitoring.

Acknowledgment

This work was supported by the National Natural Science Foundation of China under Grant 62003004.

References

[1] D. Zhou, Y. Y, Modern Fault Diagnosis and Fault Tolerant Control, Tsing Hua University Publishing House: Beijing, 2000.

[2] K. E. S. Pilario, Y. Cao, Canonical variate dissimilarity analysis for process incipient fault detection, IEEE Transactions on Industrial Informatics 14 (12) (2018) 5308–5315.

[3] K. E. S. Pilario, Y. Cao, M. Shafiee, Mixed kernel canonical variate dissimilarity analysis for incipient fault monitoring in nonlinear dynamic processes, Computers & Chemical Engineering 123 (2019) 143–154.

[4] Q. Jiang, D. S. X, Y. Wang, X. Yan, Data-driven distributed local fault detection for large-scale processes based on the ga-regularized canonical correlation analysis, IEEE Transactions on Industrial Electronics 64 (10) (2017) 8148–8157.

TABLE 3
The fault detection performance (%) for CSTR process.

No.	PCA		SMD			WD		CS		
	T^2	SPE		MD_z	MD_e	W_z	W_e		CS_z	CS_e
f_1	46.86	0.50	97.93	97.43	96.14	95.50	98.64	97.71	94.93	**99.86**
	22.88	1.99	25.49	**0**	4.90	**0**	**0**	**0**	**0**	**0**
	1	246	28	37	55	64	20	33	71	**3**
f_2	69.50	47.86	76.86	75.21	75.36	71.36	76.64	69.93	69.50	**85.71**
	23.88	0.50	8.82	23.53	**0**	**0**	**0**	**0**	**0**	**0**
	10	59	**10**	133	346	382	235	419	33	**33**
f_3	84.14	2.43	94.28	87.28	**96.35**	69.35	89.57	85.78	70.71	93.93
	19.40	0.49	**0**	**0**	**0**	**0**	**0**	**0**	**0**	**0**
	4	79	57	86	**52**	427	147	200	360	**19**
f_4	80.85	49.07	90.07	90.21	**95.93**	73.71	87.57	81.21	76.64	90.96
	27.36	0.49	**0**	**0**	**0**	**0**	**0**	**0**	**0**	**0**
	8	62	110	137	**58**	344	175	237	326	129
f_5	83.36	89.36	94.85	**95.43**	85.93	94.91	93.29	94.64	**94.93**	93.29
	27.86	0.49	**0**	0.98	**0**	**0**	**0**	**0**	**0**	**0**
	1	64	73	65	198	72	95	76	**72**	**8**
f_6	80.00	92.78	96.29	**97.29**	89.50	97.28	89.14	96.71	96.57	89.71
	19.40	1.49	**0**	**0**	**0**	**0**	**0**	**0**	**0**	**0**
	3	49	53	**39**	146	39	151	50	49	145
f_7	27.86	48.07	85.93	83.07	29.79	89.43	50.86	**92.36**	91.71	61.50
	24.87	1.49	**0**	**0**	**0**	**0**	**0**	**0**	**0**	**0**
	2	67	64	153	566	124	558	**82**	83	**44**
f_8	89.93	25.14	94.92	93.21	98.86	88.43	92.79	93.07	89.21	**94.71**
	23.38	0.99	2.94	**0**	6.86	**0**	**0**	**0**	**0**	**0**
	14	211	71	92	17	163	102	**11**	147	**75**
f_9	92.57	38.14	3.64	93.64	**98.86**	89.57	93.86	92.64	89.29	95.29
	27.36	**0**	**0**	**0**	**0**	20.59	**0**	**0**	**0**	**0**
	8	130	419	86	**17**	146	87	104	148	67
f_{10}	85.50	11.79	90.42	93.36	95.00	87.79	**94.36**	93.57	88.50	**94.36**
	25.87	0	0.98	6.86	36.27	**0**	**0**	**0**	**0**	**0**
	2	82	135	93	71	165	**78**	91	45	**78**
Ave.FDR	74.06	40.51	82.52	**90.61**	86.17	85.74	77.67	89.76	86.20	**89.93**
Ave.FAR	24.23	0.79	3.82	3.14	4.80	2.06	**0**	**0**	**0**	**0**
Ave.FDD	5	104	102	92	152	192	164	130	133	**60**

The window lengths are all set as the commonly used 100. The significance level is set as 1%. MD_z, MD_e, W_z, W_e and CS_z, CS_e denote statistic patterns of principal and residual space in statistics Mahalanobis distance, Wasserstein distance and CS divergence based framework respectively.

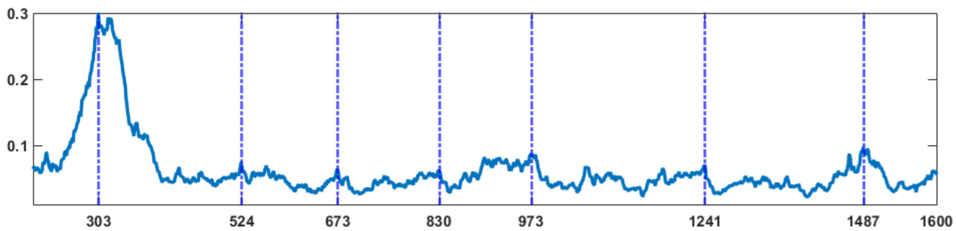

(a) Conditional CS based change point detection of f_1.

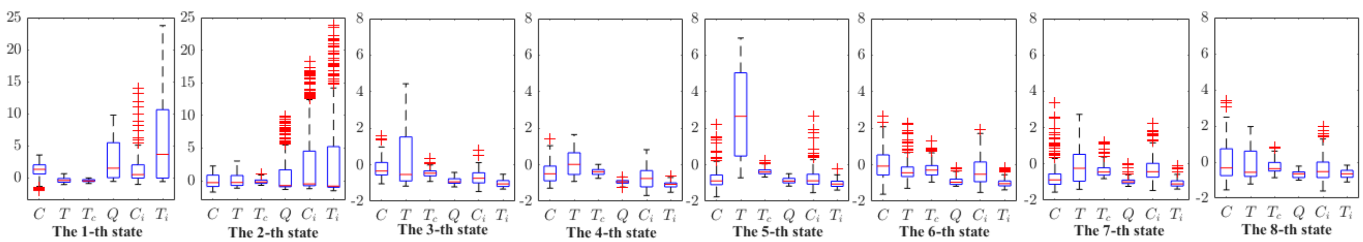

(b) Variable distribution for each state split by change points.

Fig. 3. The results of process monitoring based on change point detection of f_1 for CSTR process.(a) Conditional CS based change point detection of f_1. The vertical lines indicate the change time of next state. (b) Variable distribution for each state split by change points.